

Amino Acid Exchanges in the Putative Nuclear Export Signal of Adenovirus Type 5 L4-100K Severely Reduce Viral Progeny due to Effects on Hexon Biogenesis

Orkide O. Koyuncu,* Thomas Speiseder, Thomas Dobner, Melanie Schmid*

Heinrich Pette Institute for Experimental Virology, Hamburg, Germany

The adenovirus type 5 nonstructural L4-100K protein is indispensable for efficient lytic infection. During the late phase, L4-100K promotes selective translation of viral late transcripts and mediates the trimerization of the major capsid protein hexon. In the present study, the role of a potential nuclear export signal in L4-100K was investigated. Intriguingly, amino acid substitutions in this sequence resulted in severely diminished progeny virus production, seemingly by precluding proper hexon biogenesis.

An efficient infectious cycle of human adenovirus type 5 (Ad5) is ensured by several regulatory proteins that provide an optimal environment for replication. Processes such as gene expression, DNA replication, and assembly of the virion are mediated by these proteins (1). One of the regulatory proteins, L4-100K, is expressed during the late phase of infection from the major late transcription unit (MLTU) and is crucial for the viral life cycle (2). L4-100K not only inhibits host cell protein synthesis and ensures late viral protein production (3) but also plays an important role during capsid assembly by mediating trimerization of the major capsid protein hexon (4–6).

In 2000, an HIV-1 Rev-like nuclear export signal (NES) between amino acids 383 and 392 of the L4-100K protein was reported (7). The consensus amino acid sequence implies a high conservation of this motif among different adenovirus serotypes (Fig. 1A). Interestingly, transfection of a plasmid encoding an L4-100K with a mutated NES resulted in nuclear restriction of the protein (8). Assuming that the cytoplasmic localization of L4-100K might be critical for its multiple functions during replication, such as protein translation and hexon trimerization that take place in the cytoplasm, we aimed to determine the effect of such amino acid substitutions in L4-100K on virus replication.

Therefore, we generated an Ad5 mutant virus carrying amino acid exchanges exactly as described by Cuesta et al. (8). To introduce these L4-100K point mutations, oligonucleotide primers L4-100K-NESf (5'-CCAACGTGGAGGCTGCAACGCGGTCTCC TACGCTGGAGCTTTGCACGAAAACCGC-3') and L4-100K-NESr (5'-GCGGTTTTCTGCAAGCTCCAGCGTAGGAGAC CGCGTTGCAGGCTCCACGTTGG-3') were used for site-directed mutagenesis of the L4-100K box in pL4-1513 (9), resulting in pL4-1548. This box was inserted into pH5pm4100 by SpeI/SgfI digestion to generate adenoviral bacmid pH5pm4165 (9). Transfection of the viral genome into the L4-100K-complementing cell line K16 (10) repeatedly failed to generate L4-100K mutant virus, perhaps due to the inadequate ectopic expression of the viral gene or, possibly, dominant-negative inhibition of wild-type (wt) L4-100K protein via dimerization with the mutant L4-100K. Therefore, we used 2E2 cells (11) and cotransfected pTL-flag-Ad2-100K plasmid (2) together with the linearized pH5pm4165 bacmid to produce the mutant virus. 2E2 cells, described by Catalucci et al. in 2005, are used to complement defects

in the early phase of adenoviral infection by expressing the E1 and E2 region, as well as E4orf6, under the control of a tetracycline-inducible promoter. The expression of early proteins provides an optimal environment for the late phase of adenoviral infection, and additional transfection of the wt L4-100K protein allowed us to produce the L4-100K mutant virus. To be able to obtain a high-titer virus stock, we performed several rounds of reinfections.

Surprisingly, virus stocks prepared in this way consistently resulted in a chimeric virus with both wt and mutated sequences (Fig. 1B). In all cases, these mixed sequences were detected not only in the mutated positions but also in the residues that differ between Ad2 and Ad5 L4-100K DNA sequences; they spanned 200 to 250 nucleotides (Fig. 1C). These observations indicated homologous recombination driven by a strong negative selection pressure against the mutant L4-100K, implying a severe defect caused by the inserted mutations.

To be able to obtain a low-titer but pure virus stock ($\sim 10^4$ particles/ μ l), we cotransfected wt L4-100K plasmid but limited the reinfection steps. The purity of the H5pm4165 virus stock was tested by a PCR-based screen in the putative NES region. Therefore, viral DNA was isolated by phenol-chloroform precipitation, and full-length L4-100K was amplified by PCR using oligonucleotide primers 100K-BamHI-fw (5'-CGGGATCCATGGAGTCAG TCGAGAAGAAGG-3') and 100K-EcoRI-rev (5'-CGGAATTCC TACGGTTGGGTCGGCGAACGGGC-3'). Then, the PCR amplicon was purified from an agarose gel (GelJet kit; Fermentas) and digested with the restriction enzyme SacI (New England Biolabs) according to the manufacturer's protocols. The DNA restriction pattern was analyzed on a 0.8% agarose gel and com-

Received 7 August 2012 Accepted 8 November 2012

Published ahead of print 21 November 2012

Address correspondence to Thomas Dobner, thomas.dobner@hpi.uni-hamburg.de.

* Present address: Orkide O. Koyuncu, Princeton University, Department of Molecular Biology, Princeton, New Jersey, USA; Melanie Schmid, European Molecular Biology Laboratory, Heidelberg, Germany.

Copyright © 2013, American Society for Microbiology. All Rights Reserved.

doi:10.1128/JVI.02061-12

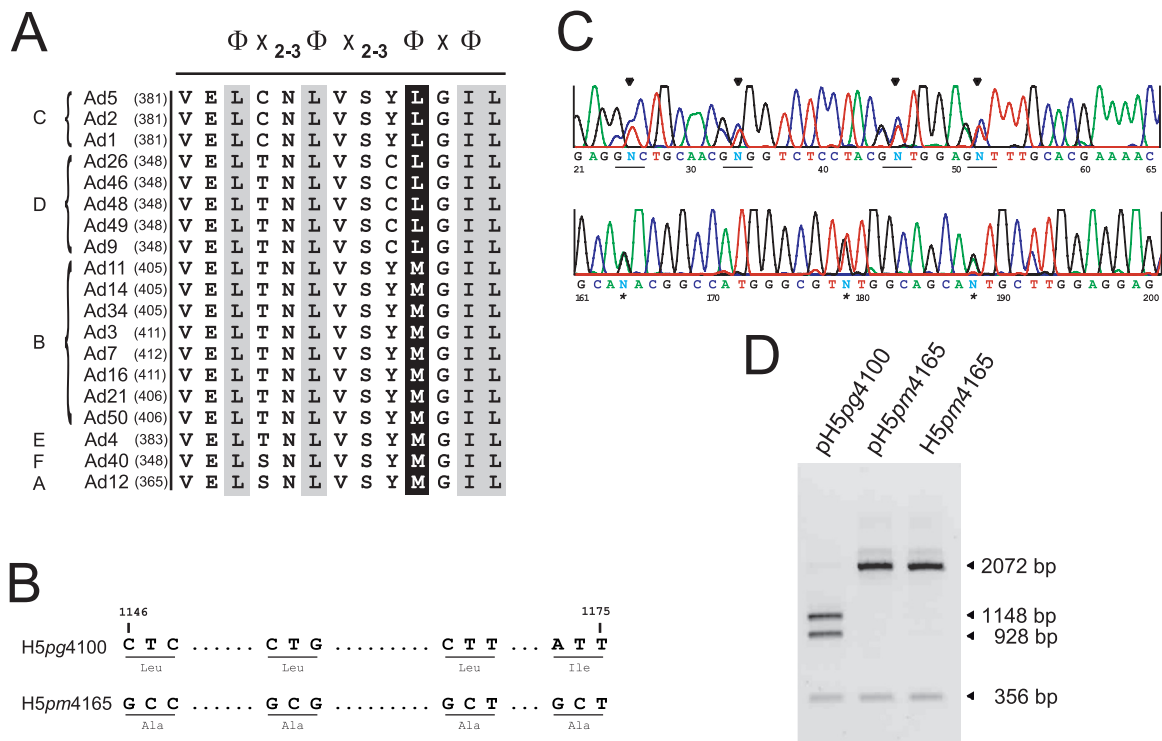


FIG 1 Negative selection against H5pm4165 by homologous recombination in H1299 cells. (A) Multiple amino acid sequence alignment of L4-100K polypeptides from different human Ad types classified into 6 subgroups (A to F) compared to the NES consensus sequence (Φ : hydrophobic amino acid residue; X: any amino acid residue). Numbers in brackets refer to the number of amino acid residues in the respective L4-100K protein. Hydrophobic residues that are identical in all types are shown in light gray boxes. The conserved hydrophobic residue is marked in a black box. (B) Nucleotide sequence of wt H5pg4100 and mutant H5pm4165 viruses. Numbers refer to positions of nucleotides in the wt L4-100K DNA sequence. Hydrophobic amino acids encoded by the underlined codons are shown below. (C) Sequencing data of an H5pm4165 virus stock generated by cotransfecting Ad2-100K plasmid. Arrowheads indicate the mixed sequence (N) of nucleotides at the positions of inserted mutations. Asterisks denote the mixed sequence of nucleotide residues that differ between Ad2 and Ad5 L4-100K DNA sequences. (D) The purity of the H5pm4165 virus stock was tested by PCR amplification and subsequent digestion of the purified amplicon with the restriction enzyme *SacI*. The DNA restriction pattern was analyzed on an agarose gel and compared to those of similarly treated wt (pH5pg4100) and mutant L4-100K (pH5pm4165) bacmid DNA.

pared to those of similarly treated wt (pH5pg4100) and mutant L4-100K (pH5pm4165) bacmid DNA. Due to the loss of a *SacI* restriction site, the DNA restriction pattern of L4-100K changes upon mutation of the putative NES (Fig. 1D, second lane). This specific restriction pattern is also displayed by the H5pm4165 mutant virus (Fig. 1D, third lane), proving the purity of the virus stock. Subsequently, this low-titer, pure L4-100K mutant virus (H5pm4165) was analyzed for viral gene expression, virus growth, L4-100K subcellular localization, and hexon trimerization.

To determine protein steady-state levels, Western blot analyses were performed from protein lysates of H5pg4100- and H5pm4165-infected A549 cells as described previously (9). To detect early E2A-72K and E1B-55K proteins, monoclonal antibodies (MAb) B6-8 (12) and 2A6 (13) were used. Late L4-100K and capsid proteins were detected with MAb 6B10 (14) and anti-Ad5 rabbit polyclonal serum L133 (15), respectively. Analyses of early protein expression (Fig. 2A) and viral DNA accumulation (data not shown) revealed no significant difference between the results of wt- and mutant-virus infection. Although the mutations in the putative NES motif resulted in less accumulation of the L4-100K protein itself, the viral capsid proteins, penton and fiber, accumulated to the same level as in wt-virus-infected cells (Fig. 2A). This demonstrated that amino acid exchanges do not affect L4-100K function in late viral protein translation. In contrast, the expres-

sion of hexon, as well as that of hexon-associated proteins (protein VI, major core protein VII, and protein VIII and IX), was reduced compared to that in the wt virus (Fig. 2A). These results indicate that although the inserted mutations do not affect early and late protein synthesis, these specific amino acids might play a role in hexon biogenesis and, consequently, affect the stability of hexon-associated proteins.

Next, we tested the virus progeny production of the L4-100K mutant in comparison to that in wt-virus-infected cells. A549 cells were infected with both mutant and wt Ad5 viruses harvested at time points indicated below, and virus yield was determined by quantitative E2A-72K staining (9). Intriguingly, our results revealed severe decreases in mutant virus growth of up to 240-fold depending on the multiplicity of infection (MOI) used and the time after infection (Fig. 2B). Unlike early gene mutants, which generally compensate defects with increased particle numbers per cell, especially at later time points (16, 17), H5pm4165 showed the strongest decreases in viral progeny in comparison to the virus progeny production of the wild type with the use of a higher MOI and later during replication (Fig. 2B). We hypothesize that inefficient hexon biogenesis of the H5pm4165 virus (Fig. 2A) limits the production of new progeny by restricting the assembly of capsids even at a high MOI. While wt virus produces higher numbers of progeny with increasing MOI and infection time, reaching a pla-

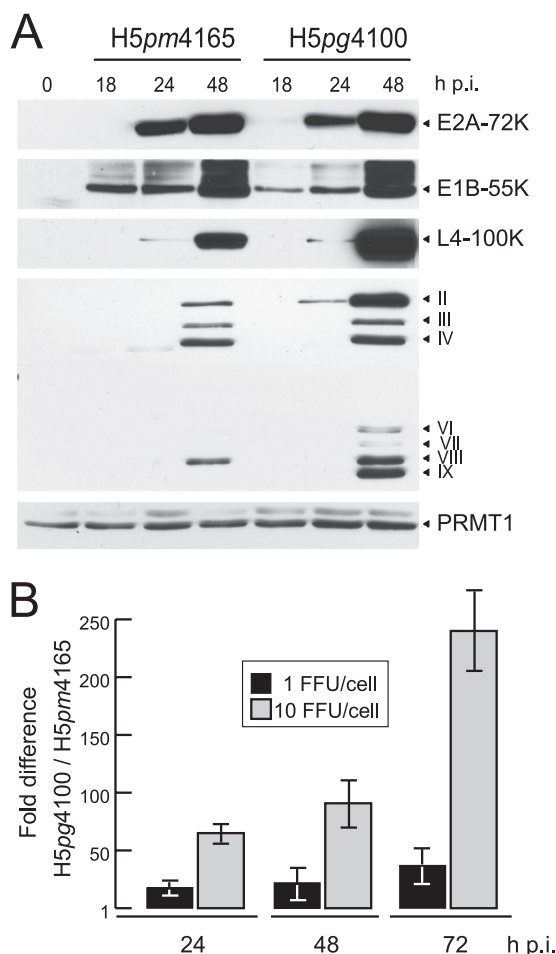


FIG 2 Effects of amino acid substitutions in L4-100K on protein synthesis and virus growth. (A) Viral protein synthesis. A549 cells were infected with the wt or mutant virus at a multiplicity of 10 focus-forming units (FFU) per cell. Total cell extracts were prepared at indicated times after infection. Proteins (25 μ g samples) were separated by SDS-PAGE, transferred to nitrocellulose membranes, and probed with mouse Mab B6-8 (E2A-72K), mouse Mab 2A6 (E1B-55K), rat Mab 6B10 (L4-100K), and anti-Ad5 rabbit polyclonal antiserum L133 and with anti-PRMT1 rabbit polyclonal antibody as a loading control. Bands corresponding to viral late proteins hexon (II), penton (III), and fiber (IV), as well as capsid-associated proteins (VI, VII, VIII, and IX), are indicated on the right. (B) Virus yield. A549 cells were infected with wt H5pg4100 or H5pm4165 at indicated multiplicities. Viral particles were harvested at indicated time points (h.p.i.) and virus yield was determined by quantitative E2A-72K immunofluorescence staining on K16 cells. The results represent the averages from three independent experiments. Error bars indicate the standard errors of the means.

teau at \sim 72 h postinfection (h.p.i.) (18), mutant virus stays at a limited yield, resulting in the noted difference later in infection, especially at a higher MOI (Fig. 2B).

So far, subcellular localization of L4-100K carrying mutations in the putative NES has only been determined by transient transfection (8). In contrast to wt L4-100K, which localizes to both the cytoplasm and nucleus (19), the mutated L4-100K protein was found predominantly in the nuclear compartment (8). We could confirm these observations in transient-transfection experiments (data not shown). However, to better understand the effect of the L4-100K NES mutations on viral replication, the subcellular localization during infection of the mutated protein in comparison to

that of the wt L4-100K protein was investigated. For this purpose, A549 cells were infected with H5pg4100 (wt) and H5pm4165 (mutant) virus. Thirty-six hours postinfection, cells were fixed with methanol and immunofluorescence analysis was performed (20), using anti-L4-100K Mab 6B10 (14). Most surprisingly, the L4-100K protein showed a predominantly cytoplasmic staining pattern in both wt- and mutant-virus-infected cells (100% of cells examined in both cases, $n = 61$ and $n = 40$, respectively) (Fig. 3A and B, compare panels a and d), with the mutated L4-100K being less abundant, in agreement with the Western blot analysis. However, while L4-100K was diffusely distributed in wt-virus-infected cells (100%, $n = 61$), the mutated protein frequently formed distinct punctate structures (Fig. 3A and B, panels d, arrowheads) in the cytoplasm in close proximity to the nuclear membrane (27.5%, $n = 40$). In contrast to the results of transient-transfection experiments (8), mutation of the potential NES in L4-100K did not lead to nuclear retention of the protein during infection.

Since L4-100K acts as a chaperone to form hexon trimers (4–6), which are subsequently imported into the nucleus by adenoviral protein VI (pVI) (21), we next tested whether both hexon and pVI are properly localized in H5pm4165-infected cells. For the costaining with L4-100K, we used antihexon rabbit polyclonal antiserum (ab123995; abcam) or anti-protein VI rabbit Mab pVI (21). In wt-virus-infected cells, functional trimerization and nuclear import of the hexon protein resulted in a predominantly nuclear staining pattern for both hexon (Fig. 3A, panels b and c) and pVI (Fig. 3B, panels b and c) in all cells examined ($n > 20$). Intriguingly, in cells infected with L4-100K-mutant virus, both hexon (Fig. 3B, panels e and f) and pVI (Fig. 3B, panels e and f) were seemingly excluded from the nucleus (100% of cells examined, $n > 20$). Furthermore, hexon and pVI localized in cytoplasmic aggregates (Fig. 3A and B, panels e and f, arrowheads), similar to the mutated L4-100K protein (Fig. 3A and B, panels d). In addition, hexon colocalized with L4-100K in these punctate structures (Fig. 3A, panel f).

To identify the hexon binding site of L4-100K, we performed a glutathione S-transferase (GST) pulldown assay. GST fusion constructs, including full-length L4-100K and fragments (F1 to F4), were cloned into pGEX4T-1 or pGEX5X-1 (Amersham Pharmacia) vectors (Fig. 4A). Recombinant proteins were expressed from these plasmids in *Escherichia coli* TOPP6 cells, and GST pulldown assays were performed as described previously (22). To provide *in vivo*-synthesized hexon H5pg4100, wt-virus-infected A549 cell lysates were used. Strong binding of hexon to L4-100K fragment F2 (amino acids 215 to 420) and less-strong binding to F4 (amino acids 614 to 806) were detected (Fig. 4C, lanes 5 and 7), whereas no interaction was seen in the GST pulldown experiments with wt L4-100K (Fig. 4C, lane 3). The latter result indicates that the wt protein fused to GST cannot interact with hexon under the conditions used.

Since the hexon binding region of L4-100K, primarily amino acids 215 to 420 (Fig. 4C), overlaps with its putative NES sequence (amino acids 383 to 392) (7), mutations in this motif might alter the regulation of L4-100K–hexon interaction, resulting in reduced hexon trimerization and, consequently, in impaired nuclear import of these trimers by pVI. To test this hypothesis, the interaction of the mutated L4-100K with hexon was determined in H1299 cells, which were first transfected with wt or NES pTL-flag-100K plasmid as described previously (23) and subsequently infected with the H5pg4100 (wt) virus. Western blot analyses dis-

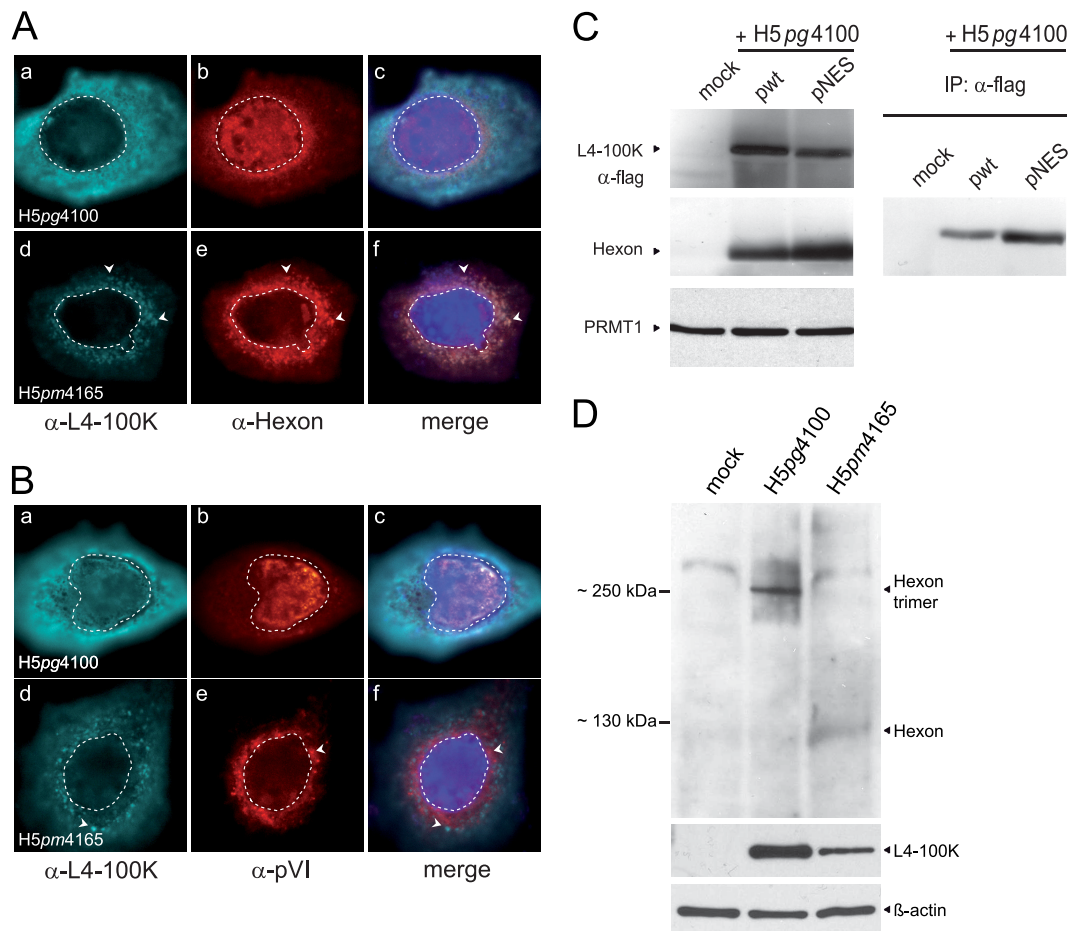


FIG 3 Effect of L4-100K NES mutation on hexon localization, binding, and trimerization. (A, B) Intracellular localization of L4-100K and hexon (A) or pVI (B) in virus-infected cells. A549 cells were infected with H5pg4100 and H5pm4165 viruses at a multiplicity of 10 FFU per cell and fixed at 36 h.p.i. Cells were labeled with anti-L4-100K rat MAb 6B10 (α -L4-100K) and anti-hexon rabbit polyclonal serum (A; α -hexon) or anti-protein VI rabbit MAb pVI (B; α -pVI), plus Cy5- and Cy3-conjugated secondary antibodies, respectively. Representative anti-L4-100K (green; a and d) and antihexon or anti-pVI (red; b and e) antibody staining patterns are shown. Overlays of DAPI (4',6'-diamidino-2-phenylindole) staining (blue) with the green and red images are shown in panels c and f (merge). Nuclei visualized using DAPI are indicated by a dashed line in all panels. Arrowheads in the images indicate L4-100K, hexon, and pVI cytoplasmic aggregates and/or L4-100K/hexon colocalization. (C) Interaction between hexon and L4-100K. H1299 cells were transfected with wt (pwt) or NES pTL-flag-100K (pNES) plasmids and infected with H5pg4100 virus (10 FFU/cell) 6 h after transfection. Total cell extracts were prepared from noninfected (mock) and transfected-infected cells 30 h.p.i. Aliquots of 25 μ g of lysates were separated by SDS-PAGE and analyzed by immunoblotting using anti-flag MAb M2, antihexon rabbit polyclonal serum, and anti-PRMT1 rabbit polyclonal antibody as a loading control. The same lysates were used for immunoprecipitation (IP) with anti-Flag MAb. The immunocomplexes were separated by SDS-PAGE and analyzed by immunoblotting using the antihexon rabbit polyclonal serum. (D) Hexon trimerization in virus-infected cells. A549 cells were infected with H5pg4100 and H5pm4165 viruses at a multiplicity of 1 FFU per cell and harvested at 48 h.p.i., and total cell extracts were prepared under native conditions. Proteins (25- μ g samples for hexon and 10- μ g samples for L4-100K and β -actin) were separated by SDS-PAGE and subjected to immunoblotting using antihexon rabbit polyclonal antiserum, anti-L4-100K rat MAb 6B10, and anti- β -actin mouse MAb AC-15. Bands corresponding to hexon monomers and/or trimers are indicated on the right.

played similar steady-state levels of hexon and flag-tagged L4-100K protein in infected cells. Interestingly, the hexon protein coimmunoprecipitated even more efficiently with the mutated L4-100K than with the wt protein. Next, to assay the trimerization efficiency of hexons, A549 cells were harvested 48 h after wt- and mutant-virus infection. L4-100K levels were determined by Western blot analysis (9) using anti-L4-100K MAb 6B10 (14). As observed earlier (Fig. 2A), mutating L4-100K resulted in reduced protein levels compared to the levels in wt-virus-infected cells. To be able to detect hexon trimers, samples were not boiled up prior to separation by 8% SDS-PAGE; separation was followed by immunostaining with antihexon antibody (ab123995; abcam). This condition, previously described for adenovirus fiber trimers (24),

allowed us to detect ~ 320 -kDa hexon trimers in the H5pg4100 (wt)-virus-infected cell sample (Fig. 3D). Intriguingly, mutations in L4-100K not only reduced hexon protein levels (Fig. 2A) but also nearly precluded hexon trimerization (Fig. 3D). The earliest analysis of hexon trimerization indicated a self-assembly mechanism of partially digested hexons (25). A low but undetectable rate of hexon trimer self-assembly during infection with the L4-100K mutant virus might provide an explanation for the production of small amounts of progeny virions (Fig. 2B).

In addition, inefficient hexon trimerization could provide an explanation for the reduced levels of hexon-associated proteins (Fig. 2A), which might rely on hexon trimers to ensure protein stability. For example, protein IX is one of the capsid proteins that

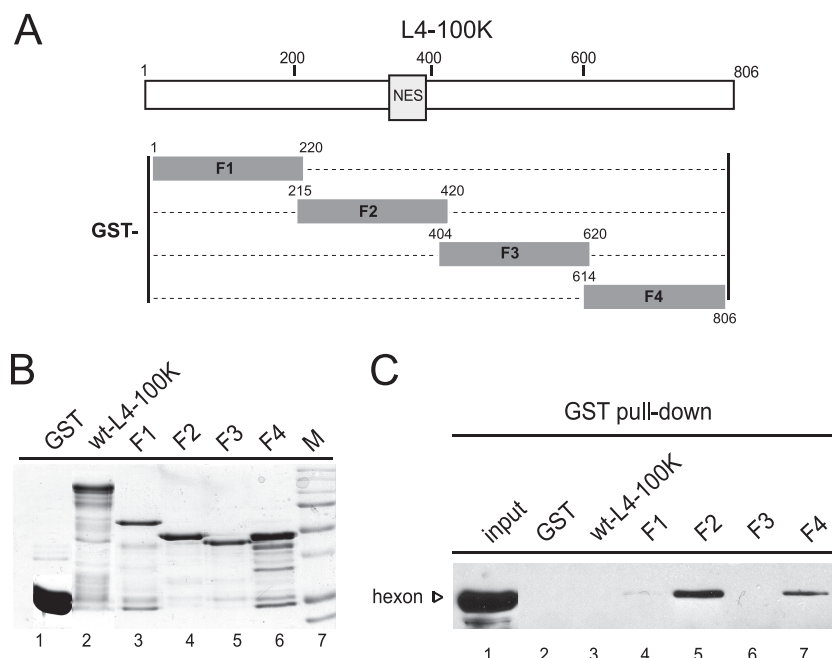


FIG 4 Mapping hexon binding regions in L4-100K. (A) Schematic diagram showing the location of the putative nuclear export signal (NES) in the L4-100K protein. GST-tagged fusion fragments of L4-100K (F1-F4) are depicted below the protein map. Numbers refer to amino acid residues of Ad5 L4-100K. (B) GST and GST-100K fragments were purified from *E. coli* using glutathione-Sepharose. Purified proteins were subjected to SDS-PAGE and Coomassie brilliant blue staining. M, molecular-weight marker. (C) H5pg4100-infected A549 cell lysates were incubated with GST or GST fusion fragments. Aliquots of 25 μ g from the cell lysates were used as input. GST-protein complexes were isolated with glutathione-Sepharose and subjected to SDS-PAGE and Western blotting with antihexon antibody.

is greatly reduced in the course of L4-100K mutant infection. This minor capsid protein associates with hexon trimers to make up the facets of the icosahedrons (26). If hexon trimers are not built effectively, the inefficient interaction between these two proteins might lead to protein IX degradation.

Taken together, the data presented here reveal a critical role for the hydrophobic residues between amino acid 383 and 392 of the regulatory L4-100K protein during adenovirus replication. This region was proposed to serve as a nuclear export signal, since the mutations in this motif led to nuclear retention of L4-100K in transient-transfection assays (8). Intriguingly, the results presented here show that these specific amino acids in L4-100K are essential for hexon biogenesis in both trimerization and nuclear import aspects. The inability of the mutated L4-100K to trimerize the capsid protein provides an explanation for the aggregation of both proteins in the cytoplasmic compartment and the simultaneous exclusion of pVI from the nucleus. This is consistent with the results of studies that identified pVI as the protein responsible for hexon trimer import (21, 27). Remarkably, L4-100K binding to hexon is enhanced in mutant-virus-infected cells. This might be due to a higher affinity of the chaperone protein to hexon monomers than to assembled hexon trimers (4). In addition, it might explain the unexpected staining pattern of L4-100K in infected cells, which is very possibly due to the unregulated hexon interaction interfering with the nuclear import of these proteins. Altogether, the mutations in the L4-100K NES motif severely reduced adenovirus growth not by causing L4-100K nuclear retention but subverting hexon biogenesis. The effect of the amino acid exchanges seemingly occurs before the import of L4-100K into the nucleus. Of note, our results suggest that nucleocytoplasmic shut-

ting of L4-100K may be regulated by hexon and a possible pVI interaction during the infection cycle. Thus, it remains unclear whether the NES motif mediates the nuclear export of L4-100K during infection, and this offers a potential starting point for future studies.

ACKNOWLEDGMENTS

We thank A. Amalfitano for K16 cells and Robert J. Schneider for plasmid pTL-flag-Ad2-100K.

This work was supported by the Erich and Gertrud Roggenbuck Foundation, Hamburg, Germany. The Heinrich Pette Institute is supported by the Freie und Hansestadt Hamburg and the Bundesministerium für Gesundheit.

REFERENCES

- Shenk T. 2001. Adenoviridae: the viruses and their replication, p 2264–2300. In Knipe DM, Howley PM (ed), *Fields virology*, 4th ed. Lippincott Williams & Wilkins, Philadelphia, PA.
- Xi Q, Cuesta R, Schneider RJ. 2004. Tethering of eIF4G to adenoviral mRNAs by viral 100k protein drives ribosome shunting. *Genes Dev.* 18: 1997–2009.
- Zhang Y, Feigenblum D, Schneider RJ. 1994. A late adenovirus factor induces eIF-4E dephosphorylation and inhibition of cell protein synthesis. *J. Virol.* 68:7040–7050.
- Cepko CL, Sharp PA. 1982. Assembly of adenovirus major capsid protein is mediated by a nonviral protein. *Cell* 31:407–415.
- Hong SS, Szolajka E, Schoehn G, Franqueville L, Myhre S, Lindholm L, Ruigrok RW, Boulanger P, Chroboczek J. 2005. The 100K-chaperone protein from adenovirus serotype 2 (subgroup C) assists in trimerization and nuclear localization of hexons from subgroups C and B adenoviruses. *J. Mol. Biol.* 352:125–138.
- Morin N, Boulanger P. 1986. Hexon trimerization occurring in an assembly-defective, 100K temperature-sensitive mutant of adenovirus 2. *Virology* 152:11–31.

7. Henderson BR, Eleftheriou A. 2000. A comparison of the activity, sequence specificity, and CRM1-dependence of different nuclear export signals. *Exp. Cell Res.* 256:213–224.
8. Cuesta R, Xi Q, Schneider RJ. 2004. Structural basis for competitive inhibition of eIF4G-Mnk1 interaction by the adenovirus 100-kilodalton protein. *J. Virol.* 78:7707–7716.
9. Koyuncu OO, Dobner T. 2009. Arginine methylation of human adenovirus type 5 L4 100-kilodalton protein is required for efficient virus production. *J. Virol.* 83:4778–4790.
10. Hodges BL, Evans HK, Everett RS, Ding EY, Serra D, Amalfitano A. 2001. Adenovirus vectors with the 100K gene deleted and their potential for multiple gene therapy applications. *J. Virol.* 75:5913–5920.
11. Catalucci D, Sporeno E, Cirillo A, Ciliberto G, Nicosia A, Colloca S. 2005. An adenovirus type 5 (Ad5) amplicon-based packaging cell line for production of high-capacity helper-independent deltaE1-E2-E3-E4 Ad5 vectors. *J. Virol.* 79:6400–6409.
12. Reich NC, Sarnow P, Duprey E, Levine AJ. 1983. Monoclonal antibodies which recognize native and denatured forms of the adenovirus DNA-binding protein. *Virology* 128:480–484.
13. Sarnow P, Sullivan CA, Levine AJ. 1982. A monoclonal antibody detecting the adenovirus type 5-E1b-58Kd tumor antigen: characterization of the E1b-58Kd tumor antigen in adenovirus-infected and -transformed cells. *Virology* 120:510–517.
14. Kzhyshkowska J, Kremmer E, Hofmann M, Wolf H, Dobner T. 2004. Protein arginine methylation during lytic adenovirus infection. *Biochem. J.* 383:259–265.
15. Kindsmüller K, Groitl P, Härtl B, Blanchette P, Hauber J, Dobner T. 2007. Intranuclear targeting and nuclear export of the adenovirus E1B-55K protein are regulated by SUMO1 conjugation. *Proc. Natl. Acad. Sci. U. S. A.* 104:6684–6689.
16. Bridge E, Medghalchi S, Ubol S, Leesong M, Ketner G. 1993. Adenovirus early region 4 and viral DNA synthesis. *Virology* 193:794–801.
17. Huang MM, Hearing P. 1989. Adenovirus early region 4 encodes two gene products with redundant effects in lytic infection. *J. Virol.* 63:2605–2615.
18. Blanchette P, Kindsmüller K, Groitl P, Dallaire F, Speiseder T, Branton PE, Dobner T. 2008. Control of mRNA export by adenovirus E4orf6 and E1B55K proteins during productive infection requires E4orf6 ubiquitin ligase activity. *J. Virol.* 82:2642–2651.
19. Gambke C, Deppert W. 1981. Late nonstructural 100,000- and 33,000-dalton proteins of adenovirus type 2. I. Subcellular localization during the course of infection. *J. Virol.* 40:585–593.
20. Kindsmüller K, Schreiner S, Leinenkugel F, Groitl P, Kremmer E, Dobner T. 2009. A 49-kilodalton isoform of the adenovirus type 5 early region 1B 55-kilodalton protein is sufficient to support virus replication. *J. Virol.* 83:9045–9056.
21. Wodrich H, Guan T, Cingolani G, Von Seggern D, Nemerow G, Gerace L. 2003. Switch from capsid protein import to adenovirus assembly by cleavage of nuclear transport signals. *EMBO J.* 22:6245–6255.
22. Müller D, Schreiner S, Schmid M, Groitl P, Winkler M, Dobner T. 2012. Functional cooperation between human adenovirus type 5 early region 4, open reading frame 6 protein, and cellular homeobox protein HoxB7. *J. Virol.* 86:8296–8308.
23. Schreiner S, Wimmer P, Sirma H, Everett RD, Blanchette P, Groitl P, Dobner T. 2010. Proteasome-dependent degradation of Daxx by the viral E1B-55K protein in human adenovirus-infected cells. *J. Virol.* 84:7029–7038.
24. Hesse A, Kosmides D, Kontermann RE, Nettelbeck DM. 2007. Tropism modification of adenovirus vectors by peptide ligand insertion into various positions of the adenovirus serotype 41 short-fiber knob domain. *J. Virol.* 81:2688–2699.
25. Boulanger PA. 1975. Adenovirus assembly: self-assembly of partially digested hexons. *J. Virol.* 16:1678–1682.
26. Boulanger P, Lemay P, Blair GE, Russell WC. 1979. Characterization of adenovirus protein IX. *J. Gen. Virol.* 44:783–800.
27. Kauffman RS, Ginsberg HS. 1976. Characterization of a temperature-sensitive, hexon transport mutant of type 5 adenovirus. *J. Virol.* 19:643–658.